Determining the properties of CaO-Al$_2$O$_3$-SiO$_2$ slags from molecular dynamics simulation

Mengyi Zhu[1]*, Jafar Safarian*[2]

1.Postdoctoral researcher, Norwegian University of Science and Technology (NTNU), Trondheim, 7491, Norway. Email: mengyi.zhu@ntnu.no
2. Professor, Norwegian University of Science and Technology (NTNU), Trondheim,7491, Norway. Email: jafar.safarian@ntnu.no

ABSTRACT

Understanding the slag composition-structure-property relationship remains challenging due to the amorphous nature of slag melts and the difficulty of high-temperature experimental investigations. Since the CaO-Al_2O_3-SiO_2 slag system is maybe the most important slag system for various high-temperature metallurgical process, the present research employed high-throughput molecular dynamics (MD) simulations on the entire composition region of the CaO-Al_2O_3-SiO_2 slag system to determine physical properties like molar volume, density, and diffusivity, structural properties such as distribution of different oxygen types for each simulated slag melt. The obtained slag properties result from the simulations displayed good consistency with experimental data, underscoring the reliability of the MD simulation as a novel tool to predict reasonable slag properties and to study slag behaviour from atomistic insight. The simulated results demonstrate a near-linear relationship between molar volume changes and composition, highlighting the predominant role of oxygen atoms, which is attributed to the significantly larger size of oxygen compared to other cations in the slag melts. This disparity in size leads to oxygen ions occupying most of the space in slags, thereby playing a major role in determining the overall molar volume. The simulation results of slag density revealed a decreasing trend with increased SiO_2 content and identified a local minimum at constant SiO_2 when Al_2O_3 content increases, also consistent with established slag density models. Furthermore, the simulated oxygen self-diffusion coefficients reveal a strong composition-structure-property relationship, where an increase in CaO content enhances slag diffusivity, while a minimum in diffusivity is observed near a CaO/Al_2O_3 ratio of unity. The diffusivity minimum also corresponding to the local viscosity maxima, indicating effective simulation of charge compensation effects and dynamic characteristics of slag melts. The simulated distribution of oxygen types in slag— bridging oxygen (BOs), non-bridging oxygen (NBOs), free oxygen (FOs), and tricluster oxygen (TOs)— reveals a composition-dependent pattern: BOs peak near CaO/Al_2O_3=1, NBOs and FOs are abundant in CaO-rich areas with NBOs peaking near the Ca_3SiO_5 composition, FOs in the CaO corner, and TOs predominantly in the Al_2O_3 corner, highlighting the complex interplay of network formers and modifiers for the charge compensation effects on the slag's structural properties. The successful application of MD simulations in this study paves the way for a powerful approach to explore the complex relationships in multicomponent slag systems and bridges the gap between mathematics modelling and experimental observations in high-temperature metallurgical processes.

INTRODUCTION

The emergence of the "big data" era attracts widespread attention from metallurgical engineering industry and academia. However, it is notoriously challenging for metallurgists to obtain a complete materials database for multicomponent slag systems by way of experiments at high temperature. Nevertheless, in the past decades, considerable attention has been paid to metallurgical slag falling within the composition-property relations. It is now well-known that slag property is strongly dependent on its microscopic structure at atomistic level.(Kondratiev et al., 2002; Mills et al., 2011; Min and Tsukihashi, 2017; Zhang et al., 2014). However, direct structure observation of slag melt remains an ongoing challenge due to the high temperature in metallurgical process. Therefore, introducing computational simulations to reveal and predict the slag composition-property relations is considerably urgent.

Molecular dynamics (MD) simulation has become an effective tool for predicting properties of multi-component glass and melts, facilitated by the development of high-quality and transferrable force field for the multi-component systems.(Bouhadja et al., 2013; Cormack et al., 2002; Guillot & Sator, 2007)

The CaO-Al_2O_3-SiO_2 slag system is renowned as the most crucial slag system in various high-temperature industrial processes. For instance, it is a key constituent in blast furnace slag, ladle slags, and continuous casting mold fluxes. Additionally, the significance of the CaO-Al_2O_3-SiO_2 slag system extends to applications in metallurgical-grade Si refining. Its crucial role also evident in other fields such as glass science and geology, highlighting its fundamental importance. Moreover, its importance was also underscored in the recent developed novel SisAl process for silicon and alumina production. (www.sisal-pilot.eu) In the SisAl process, aluminium is employed as the reducing agent for the aluminothermic reduction of a CaO-SiO_2 slag. This innovative approach leads to the

production of CaO-Al$_2$O$_3$-(low) SiO$_2$ slag and a silicon alloy, both of which are subjected to further processing to produce various grades of silicon and alumina.

Therefore, it is vital to gain a comprehensive understanding of the system, especially by determining its properties and obtaining structural information across the entire composition range. In fact, due to the lack of an electron in trivalent Al cations to stabilize the Al-O tetrahedron configuration, the known charge compensation phenomenon widely occurs in the Al$_2$O$_3$-bearing slag system. This also results in a series of intriguing phenomena in systems containing Al$_2$O$_3$, such as the viscosity maxima near the CaO/Al$_2$O$_3$=1 composition line, the amphoteric behavior of Al$_2$O$_3$, the formation of five-coordinated AlO$_5$ structural unit, and three-coordinated tricluster oxygen. Consequently, this makes the study of the classic CaO-Al$_2$O$_3$-SiO$_2$ slag system is particularly important in academia. Thus, in the present work, high-throughput MD simulations were performed on the CaO-Al$_2$O$_3$-SiO$_2$ slag system to obtain the respective high temperature properties and structural information to further explore the composition-structure-property relationship.

METHODS

High-throughput MD simulations were performed by using the LAMMPS package(Plimpton, 1995).Totally 231 slags were simulated with 5 mol% increment of each component, evenly spanning the CaO-Al$_2$O$_3$-SiO$_2$ ternary diagram. The Jakse force field was employed to simulate the entire ternary slag system, renowned for its capability to well describe the structural and dynamic properties of the ternary system in good agreement with experimental data and ab initio MD simulations. (Bouhadja et al., 2013) The force field consists of both long-range Coulombic interaction and short-range interactions, and is written as follows:

$$u_{ij}(r_{ij}) = \frac{q_i q_j}{4\pi\epsilon_0 r_{ij}} + A_{ij}exp\left(-\frac{r_{ij}\sigma_{ij}}{\rho_{ij}}\right) - \frac{C_{ij}}{r_{ij}^6}$$

where $\{i, j\} \in \{Ca, Al, Si, O\}$, and r denotes the distance between atom i and j. ϵ_0 represents the permittivity of vacuum. q_i is the effective charge of atom i, with the effective atomic charges for Ca, Al, Si, O assigned as 1.2, 1.8, 2.4, and -1.2, respectively. A_{ij}, ρ_{ij}, σ_{ij}, and C_{ij} are empirical parameters used to describe the short-range interaction between specific atoms pairs through a repulsive exponential term and an attractive 1/r^6 term. All parameters, which are composition-independent and remain the same for all slag simulations within the entire composition range of the ternary system, are listed in TABLE 1.

For each slag simulation, approximately 4000 atoms were randomly distributed within a box subject to periodic boundary conditions. The melt-quench process (Bauchy, 2014) was applied to prepare the slag simulation samples, where the system was initially equilibrated at 4000 K for 200 ps relaxation time to form the initial amorphous configuration and then cooled down to 2073 K at a cooling rate of 2 K/ps in the isothermal-isobaric NPT (Constant Number of particles, Pressure, and Temperature) ensemble. At 2073 K, the slag systems were further equilibrated in the NPT ensemble. This stage allowed the system to further adapt its volume according to the preset temperature and pressure conditions. After reaching equilibrium, the volume fluctuations of the simulated system were collected and averaged for the calculation of molar volume and density.

For the calculation of slag dynamic properties like self-diffusion coefficient, it is critical that the volume remains constant to avoid deviation in the diffusivity calculation due to compression or expansion of the system. Additionally, the canonical ensemble, also known as the NVT (Constant Number of particles, Volume, and Temperature) ensemble, regulates the temperature by controlling the velocities of atoms within the system, which may also impact the diffusivity simulation. Consequently, the NVT ensemble was employed as an intermediate stage for a smooth transition from the NPT ensemble to the final microcanonical (NVE) ensemble with constant volume and energy. Each stage of the simulation was conducted over a period of 200 ps during which the statistical average of system properties reached a steady state. Then, a final simulation run covering 1 ns was conducted in the NVE ensemble for the sampling of slag configurations and atom diffusivity calculation. It should also be noted that only the results for the composition points located inside the single liquid phase region according to the phase diagram at 2073 K were considered valid for analysis.

3

TABLE 1 –Two-body coefficients for the adopted potential.(Bouhadja et al., 2013)

Pair	$A_{ij}(eV)$	$\rho_{ij}(\text{Å})$	$\sigma_{ij}(\text{Å})$	$C_{ij}(eV\ \text{Å}^6)$
O-O	0.0120	0.263	3.6430	85.0840
O-Si	0.0070	0.156	2.5419	46.2930
O-Al	0.0075	0.164	2.6067	35.5747
O-Ca	0.0077	0.178	2.9935	42.2556
Si-Si	0.0012	0.046	1.4408	25.1873
Si-Al	0.0025	0.057	1.5056	18.8116
Si-Ca	0.0027	0.063	1.8924	22.9907
Al-Al	0.0029	0.068	1.5704	14.0498
Al-Ca	0.0032	0.074	1.9572	17.1710
Ca-Ca	0.0035	0.080	2.3440	20.9856

RESULTS AND DISCUSSIONS

Evaluation of slag properties simulation

In the MD simulation, the choice of the potential function is of great importance, as it directly influences the accuracy of the simulation results. Consequently, it is also essential to validate these results. The accuracy of adopted potential was firstly verified by comparing simulated and experimentally measured density values of 40wt%CaO-20wt%Al_2O_3-40wt%SiO_2 slag as seen in FIG 1. The selection of this slag composition is because the slag melt under this composition has a relatively large amount of experimental data available for comparison.

It is seen that density obtained from MD simulation shows a good agreement by comparing with measured data, respectively, Exp. 1 (Winterhager et al., 1966) and Exp.2 (Courtial and Dingwell, 1995), and developed density models (Courtial and Dingwell, 1999; Mills et al., 2011). Furthermore, FIG 1 also clearly demonstrates the significant advantage of using MD simulation to calculate the properties of the melt, which is the absence of high temperature limitations that often encountered in experimental measurement. The study range for physical properties can even be extrapolated to several thousand kelvins, which is extremely difficult to measure experimentally. Furthermore, MD simulations have demonstrated a very powerful ability to obtain reasonable data in a time-efficient and labour-saving manner.
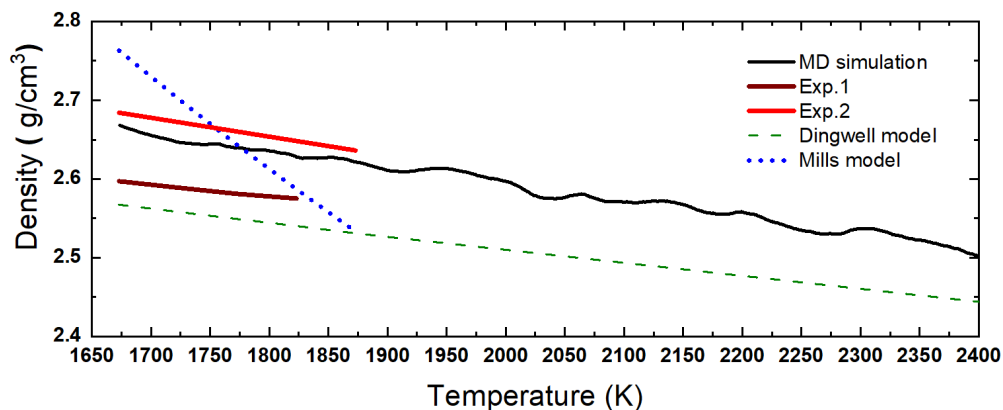

FIG 1 – Comparison of simulated and experimentally measured density of 40wt%CaO-20wt%Al_2O_3-40wt%SiO_2 slag system with varying temperature (Exp. 1 (Winterhager et al., 1966) and Exp.2 (Courtial and Dingwell, 1995)).

Another important property for evaluation of the potential function in MD simulations is the accuracy of diffusivity simulations. We have also assessed the self-diffusion coefficients of all the ions in the slag system. The results are presented in TABLE 2 and FIG 2. It can be seen that the adopted potential can effectively reflect the diffusion behaviour of ions in slag melts.

From TABLE 2, it can be seen that the self-diffusion coefficient of Ca ions obtained from simulations falls within the range of experimental measurements by different researchers. Additionally, the self-diffusion coefficients of Al and Si ions are also close to experimental results, lying within the same order of magnitude. Furthermore, the diffusion capabilities of various ions in slag melts are also clearly observed with the trend: $D_{Ca} > D_{Al} > D_{Si}$. This is in agreement with experiments (Liang et al., 1996) and clearly demonstrates the structural characteristics of Ca as a network modifier and Al, Si as network formers, forming the complex tetrahedral networks. Furthermore, the linear relationship between the self-diffusion coefficient and the reciprocal of temperature also demonstrates the sensitivity of MD simulations to temperature, specially, the Arrhenius relationship between the self-diffusion coefficient and temperature.
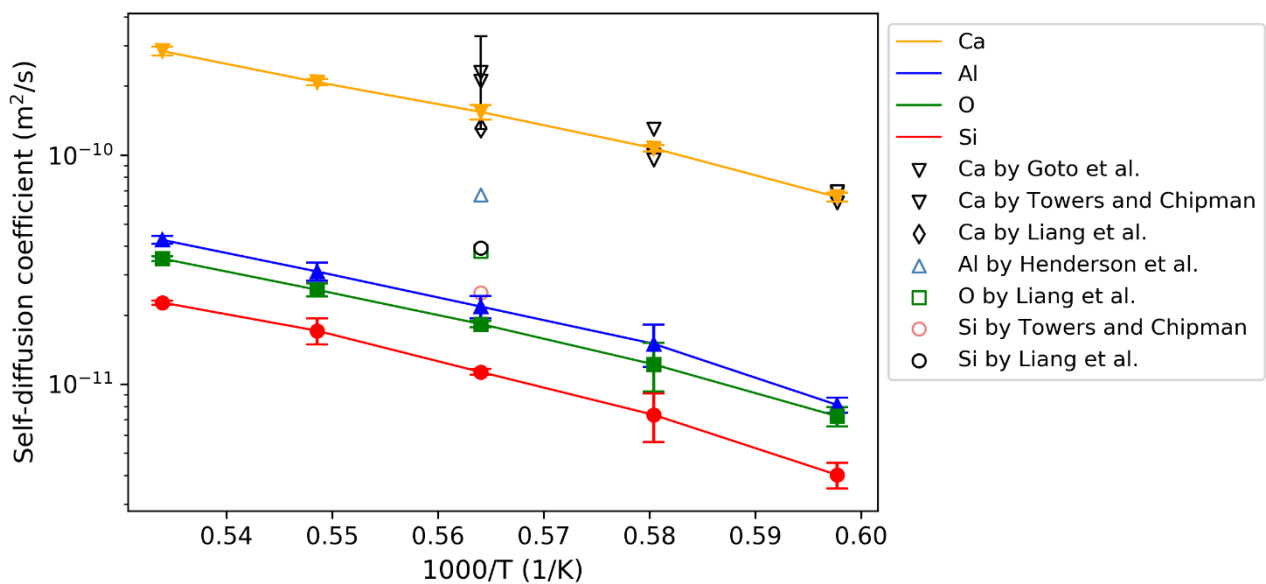

FIG 2 – Comparison of simulated and experimentally measured self-diffusion coefficients of 40wt%CaO-20wt%Al$_2$O$_3$-40wt%SiO$_2$ slag system with varying temperature.

TABLE 2- Comparison of simulated and measured self-diffusion coefficients of 40wt%CaO-20wt%Al$_2$O$_3$-40wt%SiO$_2$ under 1 atm.

Temperature [K]	D_{Ca} $\times 10^{-12} m^2 s^{-1}$	D_{Al} $\times 10^{-12} m^2 s^{-1}$	D_{Si} $\times 10^{-12} m^2 s^{-1}$	D_O $\times 10^{-12} m^2 s^{-1}$
1673 K MD	65.5±3.0	8.1±0.6	4.2±0.5	7.25±0.7
1673 K Exp.	62, 68, 69[a]			
1723 K MD	106.6±3.5	15.0±3.1	7.4±1.8	12.2±2.9
1723 K Exp.	95, 100, 130[a]			
1773 K MD	153.6±11.4	21.8±2.5	11.3±0.3	18.3±0.6
1773 K Exp.	230±100[b]; 210[a]; 131.0±4.1[d]	67[c]	25[b]; 39.2±11.0[d]	38.0±6.8[d]
[a] from Goto *et al.* (Goto et al., 1977)				
[b] from Towers and Chipman (Towers & Chipman, 1957)				
[c] from Henderson *et al.* (Henderson et al., 1961)				
[d] from Liang *et al.* (Liang et al., 1996)				

Furthermore, the structure of the melt can be accurately described with changes in its composition. As illustrated in FIG 3, the basicity has a noticeable impact on the slag structure. In slags with high basicity, B=1.2 of 50wt%CaO-10wt%Al$_2$O$_3$-40wt%SiO$_2$, there are more depolymerized areas, and the network structure formed by network formers is mainly in simple chain forms. However, with the reduction of slag basicity, B=0.8 of 40wt%CaO-10wt%Al$_2$O$_3$-50wt%SiO$_2$, the melt structure becomes more complex, resulting in a higher number of complex polyhedral ring configurations.

● Oxygen   ● Silicon   ● Aluminum   ● Calcium

Basicity=1.2   Basicity=0.8

FIG 3 – Structural visualization of depolymerized slag (left) and polymerized slag (right) with varying basicity (CaO/SiO$_2$ ratio).

High-throughput simulation results

The results of molar volume obtained through high-throughput MD simulations are shown in FIG 4. It can be observed that the molar volume changes of slag melts exhibit almost linear relationship with the composition. This indicates that the changes in the melt structure have a minor impact on the molar volume. In fact, this is because the radii of O^{2-}, which is about 1.40 Å, are much larger than those of other cations, such as Si^{4+}, which is only 0.40 Å, almost 3.5 times smaller. This means that the space occupied by one oxygen anion is about 40 times that of a Si^{4+} cation. In other words, although the ball-stick model is often used to describe the structure of slag melts, in fact, nearly 90% of the space in slag melts is occupied by oxygen anions. As for the cations, they are more like fillers in the gaps between the oxygen anions. Therefore, we can see that the primary influencing factor of molar volume is the number of oxygen atoms, particularly the content of Al$_2$O$_3$, because 1 mol of alumina provides 3 mol of oxygen anions. Additionally, an empirical rule can also be proposed: the contribution of 2 mol% SiO$_2$ to the molar volume is equivalent to the sum of 1 mol% CaO and 1 mol% Al$_2$O$_3$ due to the oxygen atomic stoichiometric coefficients are identical. Certainly, it's undeniable that due to the non-ideality of the melt structure, deviations from the near-linear relationship can occur in regions with strong structural interactions. For instance, the presence of tricluster oxygen in areas with low SiO$_2$ and low CaO content can lead to a molar volume that is smaller than the ideal scenario. However, it can be ascertained that the most significant contribution to the molar volume comes from the oxygen ions, which are not only the most abundant ion but also occupy the largest volume in the melt. This explains why numerous models for calculating slag molar volume are effective when they employ a simple linear additive function based on the partial molar volumes of individual slag components.

FIG 5 shows the simulation results of slag density for the CaO-Al$_2$O$_3$-SiO$_2$ system. The calculation of density is obtained by dividing the molar mass of the slag melt by its molar volume. A clear trend can be seen that slag density decreases with increasing SiO$_2$ content. In addition, at constant SiO$_2$ content, slag density exhibits a minimum with increasing Al$_2$O$_3$ content. This trend in density variation is also consistent with the reported slag density model(Xin et al., 2017). The observed minimum in density at compositions with maximum charge compensation reflects the complex effects of charge compensation on the network structure; although Ca^{2+} ions bond closely with Al-tetrahedra to form more stable structural units, this interaction also facilitates the formation of a more complex spatial network structure, resulting in an acceleratingly increased molar volume and results in a decreased density. As the content of Al$_2$O$_3$ increases to the peraluminous area where Al$_2$O$_3$>CaO, Ca^{2+} becomes insufficient for charge compensation, leading to the formation of smaller and denser network, which consequently raises the density. The slag density local minimum phenomenon becomes more pronounced with the reduction in SiO$_2$ content and is particularly evident in the CaO-Al$_2$O$_3$ binary system where the charge compensation effect is the most intensive.

FIG 6 shows the results of obtained oxygen self-diffusion coefficients. A strong composition-structure-property relation can also be seen. No matter whether with constant SiO$_2$ or Al$_2$O$_3$ content, the network de-polymerization caused by an increase in CaO content leads to a higher slag diffusivity, and also, a lower viscosity. Therefore, it can be observed that near the Ca-rich corner, oxygen diffusivity becomes higher, which also reflects a lower viscosity at high basicity region. However, with constant SiO$_2$ content, it can be seen that with the increase in Al$_2$O$_3$ content, oxygen diffusivity initially decreases and then increases, indicating the presence of a diffusivity minimum. This also aligns with the maxima in slag viscosity obtained in experiments(Matsushita et al., 2005). Moreover, it can be seen that this diffusivity minima occurs near the composition line of CaO/Al$_2$O$_3$=1, which clearly suggests that the potential function used in this work is capable of effectively simulating the occurrence of charge compensation effects and reflects the dynamic characteristics of the slag melt.
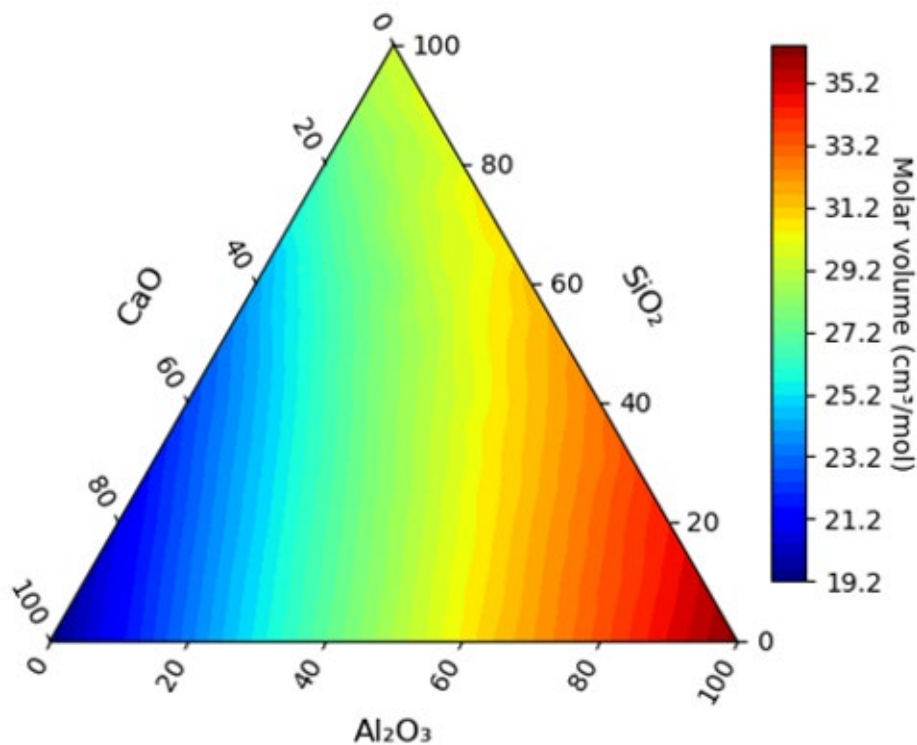

FIG 4 – Simulated molar volume values of CaO-Al$_2$O$_3$-SiO$_2$ slag system at 2073K. Note that the region outside liquid slag area corresponds to the amorphous state.
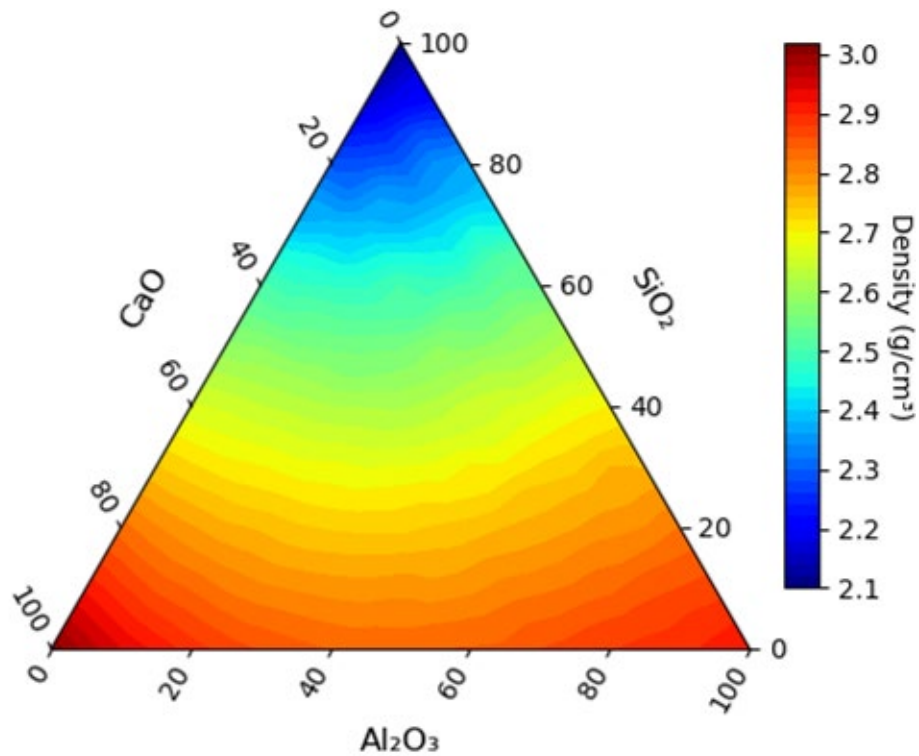
FIG 5 – Simulated density values of CaO-Al$_2$O$_3$-SiO$_2$ slag system at 2073K. Note that the region outside liquid slag area corresponds to the amorphous state.
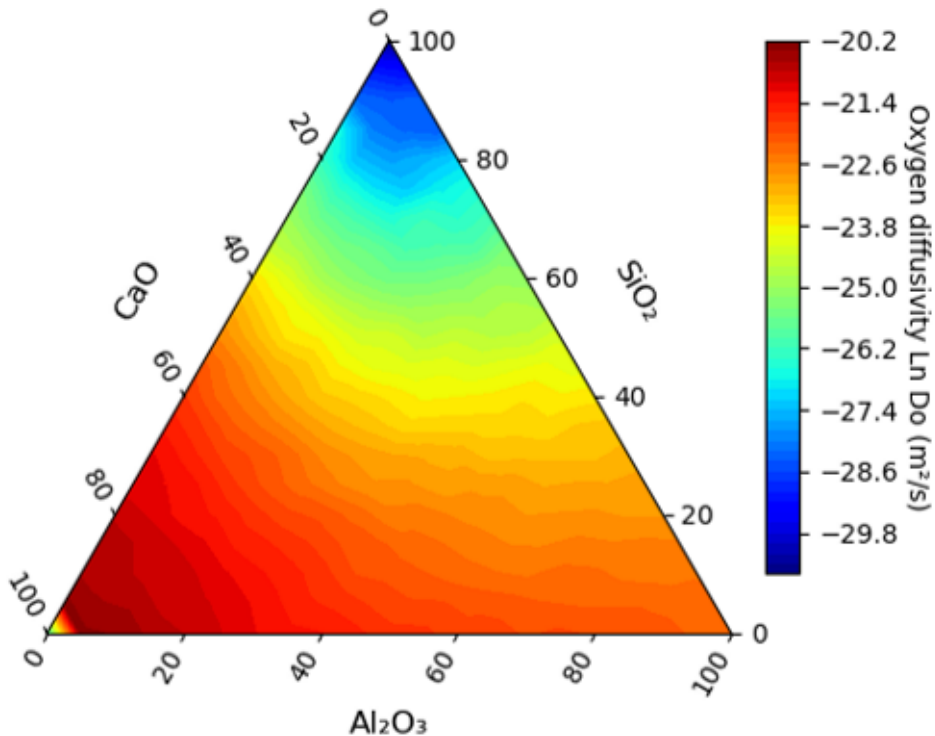

FIG 6 – Simulated oxygen self-diffusion coefficient values of CaO-Al$_2$O$_3$-SiO$_2$ slag system at 2073K. Note that the region outside liquid slag area corresponds to the amorphous state.

It is known that the slag structure could be described as a 3D amorphous network topology composed by a number of [SiO$_4$] and [AlO$_4$] tetrahedral units which connect with each other through bridging oxygen (BO). Other cations behave as a network breaker to depolymerize the chains and

to create non-bridging oxygen (NBO). The rest parts oxygen atoms are known as free oxygen (FO) and the tricluster oxygen (TO) where one oxygen is coordinated with three network formers. In this work, we have also obtained the distribution of various types of oxygen, as shown in FIG 7.

It can be observed that the distribution of these four types of oxygen shows sensitivity to the slag composition. For BOs, their local maxima appear near the compositional line of $CaO/Al_2O_3 = 1$, fully reflecting the impact of charge compensation effects on the melt structure. Under the fully charge compensation, the melt structure is the most polymerized, and also corresponding to the occurrence of the maximum viscosity. For NBOs and FOs, they are more enriched in the CaO corner, as this area contains more Ca^{2+} acting as a network modifier. Additionally, it can be seen that the peak region for NBOs appears around $CaO/SiO_2 = 3$, which corresponds to the binary compound Ca_3SiO_5, the closest binary compound to CaO in the $CaO-SiO_2$ system. As for the distribution of TOs, it is also evident that they are predominantly concentrated in the Al_2O_3 corner due to the lack of Ca cation charge compensation.
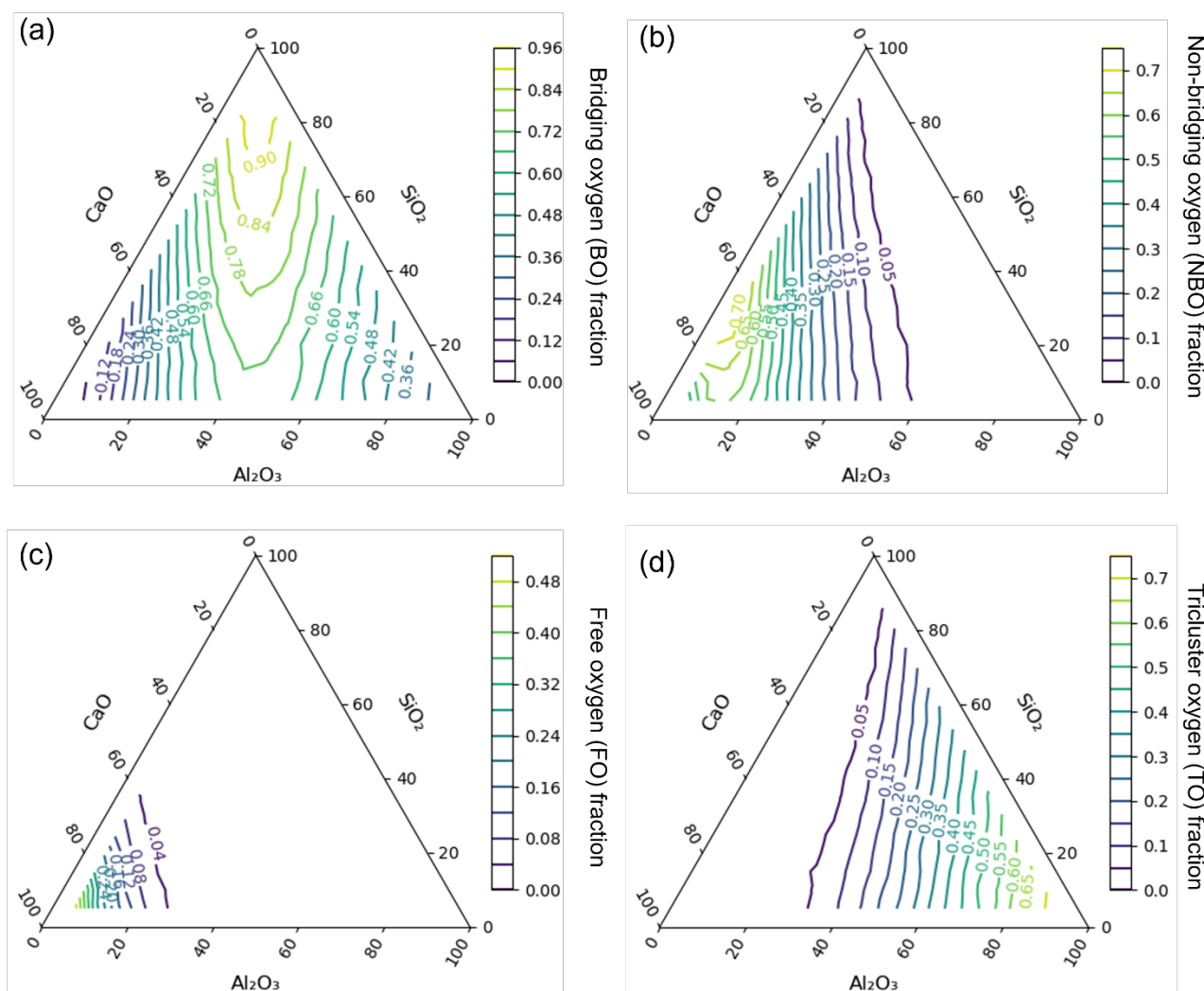

FIG 7 – Distribution of simulated oxygen types in the $CaO-Al_2O_3-SiO_2$ slag system at 2073K: (a) BO, (b) NBO, (c) FO, (d) TO. Note that the region outside liquid slag area corresponds to the amorphous state.

CONCLUSIONS

In the present work, high-throughput MD simulations were performed on the $CaO-Al_2O_3-SiO_2$ system to obtain high temperature properties and decipher the composition-structure-property relationship. The simulated density and diffusivity show a good agreement with experimental results and demonstrate the promising feature of MD simulations for the slag database development. The distribution of different oxygen types further illuminated the structural characteristics of the slag, showcasing the critical role of Ca as a network modifier and charge compensator, Si and Al as

9

network formers. This study not only provide a wealth of slag properties data on the CaO-Al$_2$O$_3$-SiO$_2$ ternary system, but also highlights the effectiveness of MD simulations in bridging the gap between theoretical predictions and experimental observations in high-temperature metallurgical processes.

ACKNOWLEDGEMENTS

REFERENCES

Bauchy, M. (2014). Structural, vibrational, and elastic properties of a calcium aluminosilicate glass from molecular dynamics simulations: The role of the potential. *Journal of Chemical Physics*. https://doi.org/10.1063/1.4886421

Bouhadja, M., Jakse, N., & Pasturel, A. (2013). Structural and dynamic properties of calcium aluminosilicate melts: A molecular dynamics study. *The Journal of Chemical Physics*, *138*(22), 224510. https://doi.org/10.1063/1.4809523

Cormack, A. N., Du, J., & Zeitler, T. R. (2002). Alkali ion migration mechanisms in silicate glasses probed by molecular dynamics simulations. *Physical Chemistry Chemical Physics*, *4*(14), 3193–3197. https://doi.org/10.1039/B201721K

Courtial, P., & Dingwell, D. B. (1995). Nonlinear composition dependence of molar volume of melts in the CaO-Al203-SiOz system. In *Geochimica et Cosmochimica Acta* (Vol. 59, Issue 18).

Courtial, P., & Dingwell, D. B. (1999). Densities of melts in the CaO-MgO-Al2O3-SiO2 system. *American Mineralogist*, *84*(4), 465–476. https://doi.org/10.2138/AM-1999-0401/MACHINEREADABLECITATION/RIS

Goto, K. S., Sasabe, M., & Kawakami, M. (1977). Relation between Tracer Diffusivity and Electrical Conductivity on Multi-component Oxide Slags at 900° to 1600°C. *Transactions ISIJ*, *17*, 212–214.

Guillot, B., & Sator, N. (2007). A computer simulation study of natural silicate melts. Part I: Low pressure properties. *Geochimica et Cosmochimica Acta*, *71*(5), 1249–1265. https://doi.org/10.1016/J.GCA.2006.11.015

Henderson, J., Yang, L., & Derge, G. (1961). Self-diffusion of aluminium in CaO-SiO2-Al2O3 Melts. *Transactions of the Metallurgical Society of. AIME. 221*, 56–60.

Kondratiev, A., Jak, E., & Hayes, P. C. (2002). Predicting slag viscosities in metallurgical systems. *JOM*, *54*(11), 41–45. https://doi.org/10.1007/BF02709749/METRICS

Liang, Y., Richter, F. M., Davis, A. M., & Watson, E. B. (1996). Diffusion in silicate melts: I. Self diffusion in CaO-Al203-SiO2 at 1500°C and 1 GPa. *Geochimica et Cosmochimica Acta*, *60*(22), 4353–4367.

Matsushita, T., Hayashi, M., & Seetharaman, S. (2005). Thermochemical and thermophysical property measurements in slag systems. *International Journal of Materials and Product Technology*, *22*(4), 351–390. https://doi.org/10.1504/IJMPT.2005.006464

Mills, K. C., Yuan, L., & Jones, R. T. (2011). *Estimating the physical properties of slags*. *111*(March), 6–9.

Min, D. J., & Tsukihashi, F. (2017). Recent advances in understanding physical properties of metallurgical slags. *Metals and Materials International 2017 23:1*, *23*(1), 1–19. https://doi.org/10.1007/S12540-017-6750-5

Plimpton, S. (1995). Fast Parallel Algorithms for Short-Range Molecular Dynamics. *Journal of Computational Physics*, *117*(1), 1–19. https://doi.org/10.1006/JCPH.1995.1039

Towers, H., & Chipman, J. (1957). Diffusion of Calcium and Silicon in a Lime-Alumina-Silica Slag. *JOM*, *9*(6), 769–773. https://doi.org/10.1007/BF03377932

Winterhager, H., Greiner, H. L., & Kammel R. (1966). *Investigations of the Density and Electrical Conductivity of Melts in the System CaO-Al2O3-SiO2 and CaO-MgO-Al2O3-SiO2* (Vol. 23). Westdeutscher Verlag.

Xin, J., Gan, L., Jiao, L., & Lai, C. (2017). Accurate density calculation for molten slags in SiO2-Al2O3-CaO-MgO systems. *ISIJ International*, *57*(8), 1340–1349. https://doi.org/10.2355/isijinternational.ISIJINT-2017-070

Zhang, G. H., Chou, K. C., & Mills, K. (2014). A structurally based viscosity model for oxide melts. *Metallurgical and Materials Transactions B: Process Metallurgy and Materials Processing Science*, *45*(2), 698–706. https://doi.org/10.1007/S11663-013-9980-Z/TABLES/11